Modeling of Friction Force based on Relative Velocity between Liver Tissue and Needle for Needle Insertion Simulation

Yo Kobayashi, *Member, IEEE,* Takahiro Sato and Masakatsu G. Fujie, *Member, IEEE*

Abstract— **Needle insertion treatments require accurate placement of the needle tip into the target cancer. However, it is difficult to insert the needle into the cancer because of cancer displacement due to the organ deformation. Then, a path planning using needle insertion simulation to analyze the deformation of the organ is important for the accurate needle insertion. A frictional model for needle insertion simulation is presented in this report. In particular, we focus on a model of frictional force based on the relative velocity between the needle and liver tissue ranging from hyper slow velocity. First, in vitro experiments using hog liver were performed at several relative velocities in order to measure the velocity dependence of the frictional force. Several needle insertion experiments were performed under identical conditions in order to deal with the variance of experimental data. The 60 frictional force data were used to obtain average data at each relative velocity. Second, the model of frictional force was developed using the averages of the experimental results. This model is defined according to the relative velocity ranging from hyper slow velocity. Finally, an evaluation experiment was carried out. The data obtained by the evaluation experiment reveals that the frictional force changes according to the relative velocity between the needle and liver tissue. The experimental results support the validity of proposed model of frictional force.**

A. Percutaneous therapy and needle insertion robot

Percutaneous therapy has gained attention as a cancer treatment method. For example, Percutaneous Ethanol Injection Therapy (PEIT) and Radio Frequency Ablation (RFA) are used to treat liver cancer. In this form of treatment, cancer cells existing inside the organ are necrotized by delivering a needle tip to the cancer cells in order to either inject ethanol (PEIT) or to ablate the cells (RFA). Percutaneous therapy has become a major trend in liver cancer treatment and has the advantages of being very minimally invasive while proving sufficient results.

In recent years, research and development have been carried out on surgical robots and navigation systems for minimally invasive and precise surgery. Research into robotic systems to assist needle insertion has also been conducted to improve the accuracy of needle placement and expand the approach path. In addition, we are developing robot assisted needle insertion systems based on the physical organ model shown in Fig. 1 [1]-[3].

In percutaneous therapy, it is necessary to accurately place the needle tip at the target cancer. Since the target organ, such as the liver, consists of soft tissue, the organ changes shape (i.e., deforms), which also changes the position of the target lesion. Therefore, it is necessary to devise a plan for the insertion path that takes organ deformation into account. A numerical simulation in a virtual surgery environment reproduced with physical models of organs may be used to create such a plan. The needle must be accurately directed to the target lesion when puncture occurs, because the needle immediately advances into the tissue after the needle punctures the liver (Fig. 2). Therefore, a correct analysis of the organ deformation and puncture occurrence is important.

B. Related research

A number of research groups have conducted studies on the development of a deformable organ model. Alterovitz et al. researched the simulation of steerable needle insertion for prostate brachytherapy [4]. DiMaio et al. developed a linear system for analyzing the extent of phantom deformation of planar tissue during needle insertion by using a linear elastic material model [5]-[6]. Dehghan et al. presented a planning system to find the optimized insertion angle and position using nonlinear organ models [7].

At the same time, a number of research groups have investigated the measurement of force information during needle insertion. Kataoka et al. investigated the relationship between needle deflection and force [8]-[9]. Abolhassani et al. investigated the needle insertion force into turkey muscle tissue and presented an online update algorithm of the needle trajectory [10]. Okamura et al. developed empirical models for the needle insertion force, comprising tissue stiffness force, friction force, and puncture force [11]-[13]. Heverly et al. showed the velocity dependency of the puncture force of biomaterial [14]. Podder et al. described the needle insertion force during prostate brachytherapy [15]. Barbe et al. investigated the online model estimation of the needle insertion force [16]-[17].

Y. Kobayashi is with Faculty of Science and Engineering, Waseda University, Japan, (59-309, 3-4-1, Ohkubo Shinjuku, Tokyo, Japan, phone: +81-3-5286-3412; fax: +81-3-5291 -8269; e-mail: you-k@fuji.waseda.jp).

T. Sato is with Graduate School of Science and Engineering, Waseda University, Japan.

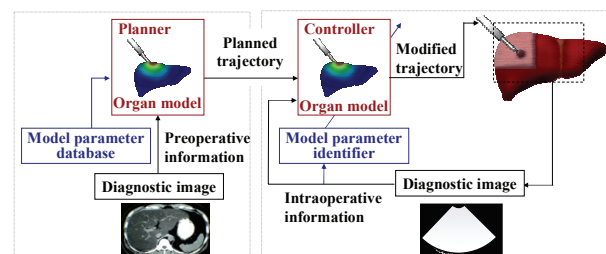M.G. Fujie is with Faculty of Science and Engineering, Waseda University, Japan.

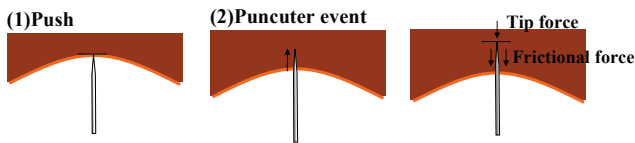Fig. 1: The needle insertion system based on physical organ model.

Fig.2. Event on needle insertion and Force condition

C. Objectives

We previously developed and reported the physical liver model, for which we provided specific descriptions of the material properties of the liver and FEM-based modeling, and presented a validation of the proposed model [1]. In addition, we reported a probability-based puncture condition [2] and a planning method based on deformation simulation of the liver and a model of the puncture conditions [3]. In this planning method, we simulated the liver deformation before the needle punctured the tissue surface. The needle insertion experiment reveals that the proposed planning method realized a needle placement accuracy of approximately 1.5 mm. Moreover it is necessary to conduct planning that includes an analysis of the situation in which the needle advances into the liver, so that the needle placement accuracy can be further improved.

The analysis including needle advancement into the liver must include frictional force in the simulation because numerous reports have revealed that the frictional force largely affects the organ deformation. Therefore, modeling of the frictional force between the organ tissue and the needle should be investigated (Fig. 2).

A number of studies have discussed the frictional properties between needle and organ tissues during needle insertion as well as the use of these properties for needle insertion simulation. However, the frictional properties included in that model are a coarse approximation of the actual friction conditions. In particular, the problem is that many frictional models are defined considering only the velocity of the needle, whereas the magnitude of the friction force is generally decided according to the relative velocity. Then, the model of friction force should be defined based on the relative velocity between the needle and organ tissue. Moreover, the friction force on the needle is distributed each contact points of needle because velocity of organ deformation varies depending on each contact points. The relative velocity near the needle tip is assumed to be low, while the relative velocity far from the needle tip is high. For example, the relative velocity at the needle tip is zero except at the time of puncture. Then, the frictional force near needle tip is assumed to be very slow. Thus, evaluation of the distributed frictional force at each contact point must correspond to relative velocity from the hyper slow range.

Therefore, we focus on the measurement and modeling of the frictional force based on the relative velocity, ranging from hyper slow velocity. The remainder of the present paper is organized as follows. Section II describes the methods used to measure the frictional force and its velocity dependence. Section III presents a discussion of the modeling of frictional force considering the velocity dependence and time varying properties. Section IV validates the proposed frictional model through an in-vitro experiment. Finally, Section V presents conclusions and plans for future research.

II. METHODS

This section describes the needle insertion experiment performed to measure the frictional force applied to the needle. Moreover, we investigated the velocity dependence of the frictional force applied to the needle, ranging from hyper slow velocity. Several needle insertion experiments performed under identical conditions are necessary so that many experimental data showed significant variation.

A. Liver condition

Hog livers were cut into rectangles (thickness: 20 mm) and sandwiched by plastic plates (Fig. 3). The needle velocity was considered to be the same as the relative velocity because the plates constricted the liver deformation. Then, this setup realized the rigorous conditioning of the relative velocity between the needle and liver tissue.

B. Experimental equipment

A bevel-tip 17-gauge biopsy needle was used for the experiment. As shown in Fig. 3, the configuration of the experimental equipment was performed by a needle with a linear stage and a force sensor. The linear stage enables the realization of a degree of freedom in the direction of needle insertion, and the force sensor enables the measurement of the force applied to the needle.

C. Experimental conditions

The experiments were conducted as follows (Fig. 4):

1) Initial insertion: The needle was inserted into the experimental sample of the sliced liver at a constant velocity of 1 mm/s. The needle stopped after penetration of the sample.

2) Measurement of frictional force: After the initial insertion, the needle was translated at a constant velocity, while the experimental conditions of needle insertion velocity were set to 30 patterns ranging from 0.01 mm/s to 10 mm/s. The needle was translated 40 mm during the experiments.

The experiments were conducted with 24 hog livers, and 60 experiments were carried out for each needle insertion velocity. The force on the needle was measured during each experiment.

III. RESULTS AND MODELING

This section describes the experimental results for frictional force and its modeling based on the experimental results. The
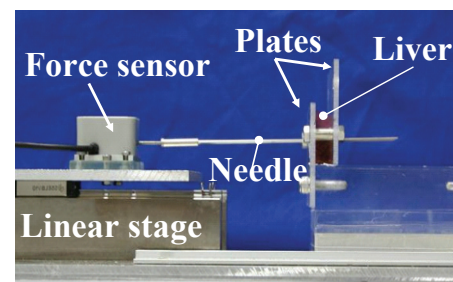

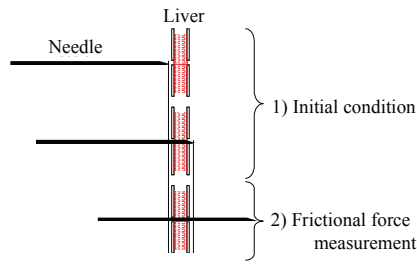Fig.3. Experimental setup to model frictional force

Fig. 4. Experimental condition used to model frictional force

Fig.6. Average of frictional force

following experimental results were obtained using 20-mm-thick sections of hog liver. The frictional force is affected by the contact length between the liver tissue and the needle. Then, considering the contact length, the following modeling of frictional force should be used in the needle insertion simulation.

A. Results and modeling of friction force

Figure 5 shows examples of the experimental results of frictional force when the needle insertion velocity was 10 mm/s. The each experimental result shows an increase in frictional force with time.

The results of the three experiments are confirmed to have a variance, although the results were obtained under the same experimental conditions. The data obtained from the experiment using living tissue tend to have a large variance. Moreover, the data of frictional force have an especially large variance. Therefore, a few samples of data is not sufficient to model the frictional force, and we should discuss the frictional force in terms of the average data. Thus, a total of 60 data of frictional force were used to obtain the average data.

Figure 6 shows an example of the average frictional force when the needle insertion velocity was 10 mm/s. The average data also show the initial frictional force and the increase in frictional force. The increase in force is assumed to originate from the viscoelastic characteristics of the liver. Then, we model the friction force on the needle using the following equation:

$$F_{friction} = F_o + at \qquad (1)$$

where $F_{riction}$ is the frictional force on the needle, F_o is the initial friction force, a is a coefficient indicating the rate of increase in force, and t is time.
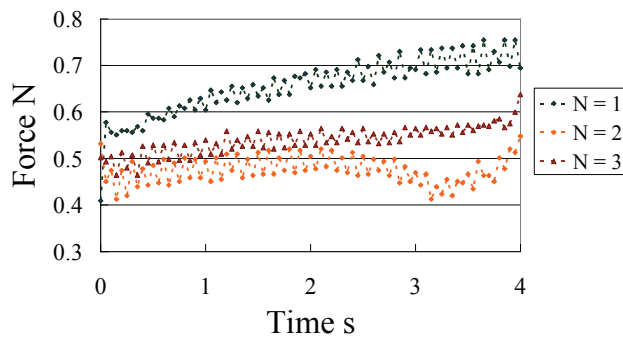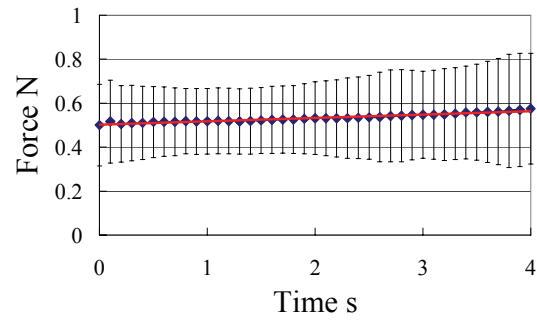
B. Modeling of velocity dependence

This section presents a discussion of the velocity dependence of the frictional force. In the following, we discuss the frictional force using relative velocity, instead of needle insertion velocity, since the relative velocity between liver and needle was the same as needle insertion velocity in this experiment.

1) Initial frictional force F_o: The initial frictional force F_o at each relative velocities were summarized through the same process described in section A. Figure 7 show the results of velocity dependence of initial frictional force F_o. The semi-logarithmic graph of Fig.7 is shown in Fig.8.

A change in tendency is found in Fig. 7 at a level of around relative velocity 1.5 mm/s. In addition, the initial frictional force F_o is considered to exhibit low-velocity characteristics when relative velocity is lower than 1.5 mm/s while high-velocity characteristics when relative velocity exceeds 1.5 mm/s. The velocity dependence of initial frictional force F_o is thus investigated using each set of results.
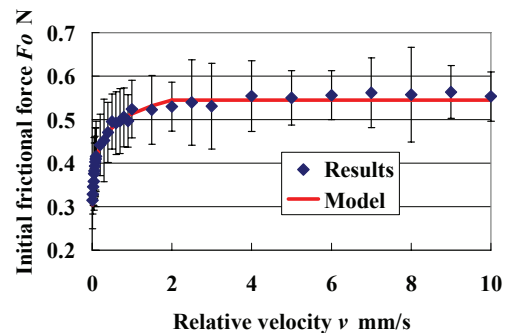

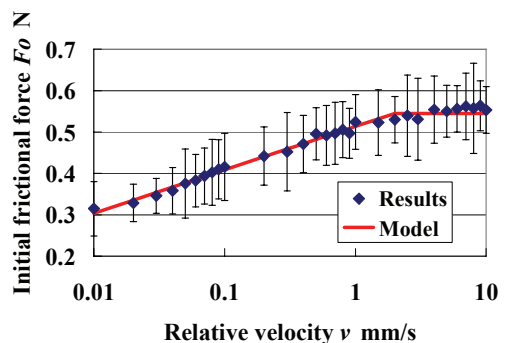Fig. 7. Velocity dependence of the initial frictional force (linear graph)

Fig. 8. Velocity dependence of the initial frictional force (semi-log graph)

Fig.5. Experimental result of frictional force

First, low-velocity characteristics are discussed from the result shown in Fig.8. The result displayed in Fig. 8 shows the initial frictional force F_o increases proportionally in the semi-log diagram during low-velocity range. Then, we modeled low-velocity characteristics using (2).

$$F_o = A\ln(v) + B \qquad (2)$$

where A and B are parameters, $ln()$ is the logarithm function, and v is the relative velocity between the liver tissue and the needle.

Second, the high-velocity characteristics are discussed based on the results shown in Fig. 7. The high-velocity frictional force is approximately constant. Then, we modeled the low-velocity characteristics using the following equation:

$$F_o = F_s \qquad (3)$$

II) Rate of increase in force, a: The rate of increase in force, a, at each relative velocity was averaged through the process described in Section III A. Figure 9 shows the velocity dependence of a. The results shown in Fig. 9 indicate that the rate of increase in force a increases proportionally as relative velocity gets higher. Then, we model the increase rate a using the following equation:

$$a = Cv \qquad (4)$$

where C is a parameter indicting the slope of the line in Fig. 9.

The frictional model depending on the relative velocity is modeled based on the above discussions using the following equation:

$$F_{friction} = \begin{cases} A\ln(v) + B + Cvt & (v < 1.5) \\ F_s + Cvt & (v \geq 1/5) \end{cases} \qquad (5)$$

IV. VALUATION EXPERIMENT

This section describes the experiment used to evaluate the model of frictional force shown in Section III. The relative velocity between the needle and the liver tissue, and the frictional force were measured. We discuss the model of frictional force based on the experimental results.
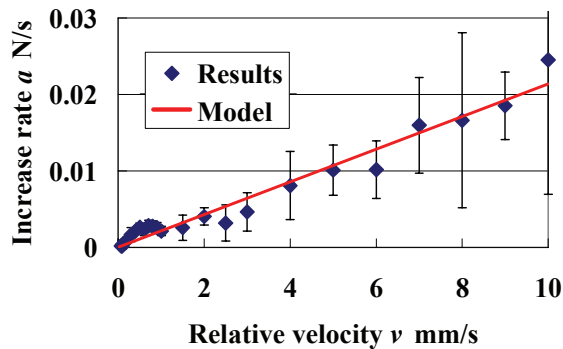

Fig.9. Velocity dependence of increase rate a

TABLE I PARAMETERS OF (5)

A	B	C	F_s
0.046	0.51	0.0021	0.55

A. Experimental method

The liver was cut into a rectangular section (thickness: 20 mm), and both sides of the liver were secured as fixed ends. Both sides of the liver were attached to sandpaper using glue, and the sandpaper was attached to the wall by double-sided tape. No rearward securing was performed (Fig. 10).

For the measurement of the relative velocity between the liver tissue and the needle, a marker was attached near the contact point of the needle and the liver tissue (Fig. 10). The position of the marker was measured, and its position was used to determine the position of the contact point through image recognition using a camera image, which was set up on the upper side of experimental table. The position of marker was used to calculate the relative velocity between the needle and the liver tissue. The experiments were conducted as follows:

1) Initial insertion: The needle was inserted into the experimental sample of the sliced liver at a constant velocity of 1 mm/s. The needle stopped after penetration of the sample.

2) Measurement of frictional force: After the initial insertion, the needle was translated at a constant velocity of 5 mm/s. A bevel-tip 17-gauge biopsy needle was used for the experiment. This is the same needle used in the experiment shown in Section II. The axial force on the needle was measured during needle insertion. The force on the needle and the marker position were measured during the experiment.

B. Results and discussions

Figure 11 shows the experimental data of liver position, relative velocity between the liver tissue and the needle, and frictional force.

The experimental results obtained during the early stage of the experiment (t < 5 s) shows that the frictional force increases nonlinearly, whereas the liver position increases linearly at the same velocity as the needle, which indicates that the relative velocity was approximately zero. In this case, the nonlinear increase in frictional force is considered to correspond to the increase in relative velocity, while this is not confirmed for low resolution data of the relative velocity due to low resolution and low update time of the camera image. This is suggested by the data shown in Fig. 7, which shows a rapid increase in frictional force during low relative velocity, ranging to 1.5 mm/s.

The experimental results during the later stage of the experiment (t > 5 s) show that the rate of increase in frictional force became small compared to the data during the early stage (t < 5 s), while the relative velocity largely increased.
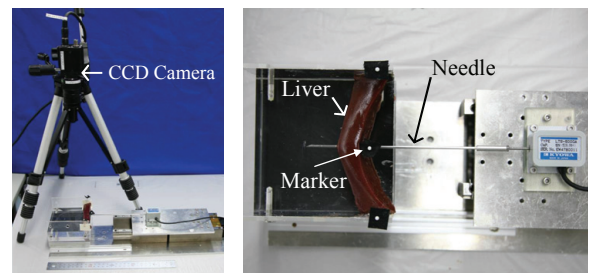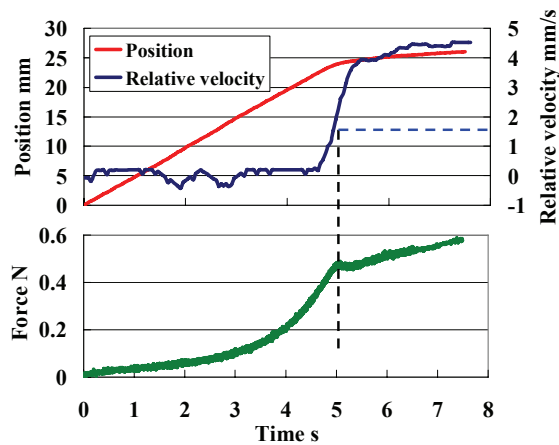

Fig.10. Setup of evaluation experiment

Fig.11. Result of evaluation experiment

In this case, the increase in force ceases because the relative velocity exceeded the slow velocity range (v < 1.5 mm/s).

As described in the above discussions, the frictional force mode changed when the relative velocity between the needle and the liver tissue is approximately 1.5 mm/s. In addition, the experimental results show a rapid increase in frictional force during low relative velocity (v < 1.5 mm/s) and low rate of increase in frictional force during high relative velocity (v > 1.5 mm/s). This condition is the same as the model of frictional force proposed in Eq. (5). Then, the data for this experiment support the frictional model shown in Eq. (5).

V. CONCLUSIONS AND FUTURE WORK

In the present paper, a frictional model for needle insertion simulation was described. We focused on a frictional model based on the relative velocity between the needle and liver tissues ranging from hyper slow velocity. First, in vitro experiments using hog liver were performed at several relative velocities in order to measure the velocity dependence of frictional force. Several needle insertion experiments were performed under identical conditions in order to deal with the variance of the experimental results. The 60 frictional force data were used to obtain average data for each needle insertion velocity. Second, a frictional force model was developed from the experimental results. The proposed model is defined using the relative velocity and the range from hyper slow velocity. Finally, an evaluation experiment was carried out. The data obtained in the evaluation experiment shows that the frictional force changes corresponding to the relative velocity between the needle and liver tissue. In addition, the experimental results support the proposed frictional model.

In the future, the frictional force model will be used in needle insertion simulation and a planning method will be proposed to realize more accurate analysis. Moreover, a model parameter identification method using intra-operative information will be investigated, with reference to the ambiguity of the model parameter. Finally, an integrated robotic system as shown in Fig.1 will be developed for use in safe and precise clinical treatment.

REFERENCES

[1] Y. Kobayashi, A. Onishi, T. Hoshi, K. Kawamura and M. G. Fujie, "In Vitro Validation of a Viscoelastic and Nonlinear Liver Model for Needle Insertion", in Proceedings of 2008 IEEE Biomedical Robotics and Biomechatronics, pp.469-476, 2008

[2] Y. Kobayashi, A. Onishi, T. Hoshi, K. Kawamura and M. G. Fujie, "A Study on Modeling of Conditions where Punctures Occur during Needle Insertion with considerations of Probabilistic Distribution", in Proceedings of 2008 IEEE International Conference on Intelligent Robots and Systems, pp.1433-1440 ,2008

[3] Y. Kobayashi, A. Onishi, H. Watanabe, T. Hoshi, K. Kawamura and M. G. Fujie, "Developing a Planning Method for Straight Needle Insertion using Probability-Based Condition where a Puncture Occurs", in Proceedings of 2009 IEEE International Conference on Robotics and Automation, (accepted)

[4] R.Alterovitz, K. Goldberg, and A. Okamura, "Planning for Steerable Bevel-Tip Needle Insertion through 2D Soft Tissue with Obstacles", In IEEE International Conference on Robotics and Automation (2005), pp.1652-1657,2005

[5] S.P.DiMaio and S.E.Salcudean "Needle Insertion Modelling and Simulation", In IEEE Transaction on Robotics and automation,Vol. 19, No. 5, pp864-875, 2003

[6] S.P.DiMaio and S.E.Salcudean "Interactive Simulation of Needle Insertion Model", In IEEE Transaction on Biomedical Engineering,Vol. 52, No. 7, pp.1167-1179, 2005

[7] E.Dehghan, S.E.Salcudean, "Needle Insertion Point and Orientation Optimization in Non-linear Tissue with Application to Brachytherapy", in 2007 IEEE International Conference on Robotics and Automation, pp.2267-2272, 2007

[8] H. Kataoka, T. Washio, M. Audette, and K. Mizuhara, "A Model for Relations between Needle Deflection, Force, and Thickness on Needle Penetration" , In proceedings of Medical Image Computing and Computer Assisted Intervention (2001), pp.966-974,2001

[9] H. Kataoka, , T. Washio, K. Chinzei, K. Mizuhara, , C. Simone, A.M.Okamura, "Measurement of the Tip and Friction Force Acting on a Needle during Penetration", In proceedings of Medical Image Computing and Computer Assisted Intervention (2002), pp. 216-23

[10] N. Abolhassani, R. Patel and M. Moallem, "Trajecory Generation for Robotic Needle Insertion in Soft Issue", In IEEE International Conference of the EMBS, pp.2730-2733, 2004

[11] C.Simone and A.M.Okamura, "Modeling of Needle Insertion Forces for Robot-assisted Percutaneous Therapy" In IEEE International Conference on Robotics and Automation (2002), pp.2085-2091,2002

[12] M.D.O'Leary, T.Washio, K.Yoshinaka, and M.Okamura "Robotic Needle Insertion:Effects of Friction and Needle Geometry", In IEEE International Conference on Robotics and Automation (2003), pp.1774-1780,2003

[13] A.M.Okamura, C.Simone and M.D.O'Leary, "Force modeling for needle insertion into soft tissue", In IEEE Transaction on Biomedical Engineering,Vol. 51, No. 10, pp.1707-1716, 2004

[14] M. Heverly, P. Dupont, J. Triedman, "Trajectory Optimization for Dynamic Needle Insertion", In IEEE International Conference on Robotics and Automation (2005), pp.1646- 1651, 2005

[15] T. K. Podder, J. Sherman, D. P. Clark, E. M. Messing, D.J. Rubens, J.G. Strang, L. Liao, R. A. Brasacchio, Y. Zhang, W.S. Ng, Y. Yu, "Evaluation of robotic needle insertion in conjunction with in vivo manual insertion in the operating room", in IEEE International Workshop on Robot and Human Interactive Communication(2005), pp. 66- 72, 2005

[16] L. Barbe , B. Bayle , M. de Mathelin and A. Gangi, "Online Robust Model Estimation and Haptic Clues Detection during In Vivo Needle Insertions", in IEEE International Confference on Biomedical Robotics and Biomechatronics (2006), pp. 341-346, 2006

[17] L. Barbe , B. Bayle , M. de Mathelin and A. Gangi, "In Vivo Model Estimation and Haptic Characterization of Needle Insertions", The International Journal of Robotics Research(2007), Vol. 26, No. 11-12, pp. 1283-1301, 2007